

Task 2.2

Title

Infrastructure adaption

Projects (presented on the following pages)

Alpine hydropower plants renewal : synergies between flexible production and hydropeaking mitigation

Mathieu Barnoud, Sabine Chamoun, Pedro Manso, Giovanni De Cesare

Suspended sediment in the turbine water of HPP Fieschertal in 2018

Matthias Eugster, David Felix, Robert Boes

Renewal of alpine hydroelectric plants according to the spatial and temporal scales of analysis

Vincent GAERTNER, Sabine CHAMOUN, Pedro MANSO, Giovanni DE CESARE

Comissioning of a new fatigue test rig based on pressure oscillations

A. Gaspoz, N. Gonçalves, L. Barras, V. Hasmatuchi, C. Nicolet, S. Rey-Mermet

Hydraulics of Horizontal Bar Rack-Bypass Systems: Field Study at HPP Stroppel

Roland Hagenbüchli, Ismail Albayrak, Mohammadreza Maddahi, Ricardo Mendez, Robert M. Boes

Two-phase flow hydraulics of low-level outlets

Benjamin Hohermuth, Lukas Schmocker, Robert Boes

Numerical investigation of HPP layouts and their effects on fish guidance racks

Andreas Huwiler

Run-up of Impulse Wave Trains

Maximilian Kastinger, Frederic Evers, Robert Boes

Assessing the acceptability of concrete dam submergence considering scour

L. Labrosse, S. Chamoun, P. A. Manso

Solving of a Lifting Problem in a Pumped Storage Power Plant

Daniel Pace, Giovanni De Cesare, Pedro Manso, Kaspar Vereide, Livia Pitorac, Leif Lia

Renewal of the Ritom hydropower plant

Jakob Siedersleben, Samuel Vorlet, Giovanni De Cesare, Nicola Tatti, Urs Müller, Graziano Sangalli

Hydro-abrasion at hydraulic structures

Damiano Vicari, Dila Demiral, Ismail Albayrak, Robert M. Boes

Seismic behavior of Pine Flat concrete gravity dam using microplane damage-plasticity model

Samuel Vorlet, Pedro Manso, Giovanni De Cesare

Alpine hydropower plants renewal : synergies between flexible production and hydropeaking mitigation

Mathieu Barnoud ; Sabine Chamoun ; Pedro Manso ; Giovanni De Cesare

EPFL

Motivation

Hydropeaking is the water flow or level variations in rivers caused by hydropower exploitation. This phenomenon have negatives impacts on fauna and flora. Mitigation measures can lead to producing less and reduce production at the times that are most economically attractive. In a context where renewable energy production wishes to be increased and where operators wish to maintain their revenues, these measures are not satisfactory. This work aims to propose mitigation solution which keep production and flexibility constant or even increase them.

Methodology and indicators

Several variants and operating scenarios will be evaluated on construction cost, energy production, revenues and hydropeaking.

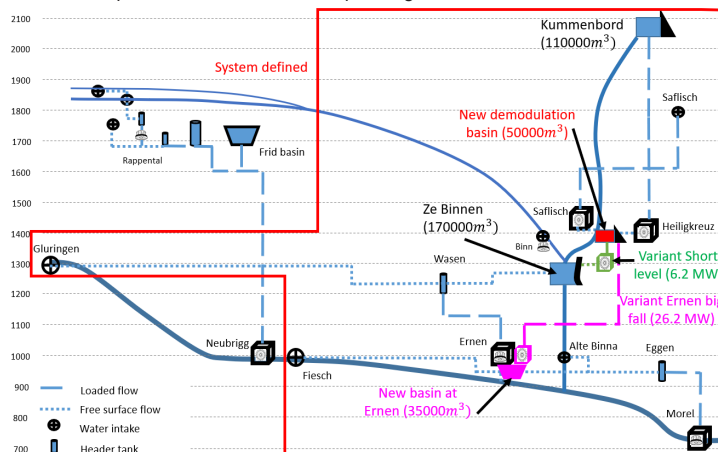
Hydropeaking will be mainly evaluated with the indicators I_A . It will be considered problematic when its value is higher than 1.5.

$$I_A = \frac{Q_t}{Q_{min}} \quad Q_t : \text{The hydropower plant exploitation discharge at time } t$$

$$Q_{min} : \text{The minimum discharge in the river on the period studied}$$

Studied case

The case study is composed of 5 hydropower plants located in the Upper-Rhône Basin. Among these installations, Heiligkreuz is subject to an order of hydropeaking sanitation. **Hydropeaking have been detected between Heiligkreuz and Ze Binnen and also downstream Mörel power plant.** Two variant were preselected and three operating scenario were studied.



Scenario Business as usual "BAU": The power plants operating modes try to be as close as possible to the reference state operating modes. The new plant operates in a similar way to Heiligkreuz one.

Scenario "Economic": The power plants use the maximum available volume when the price exceeds a threshold. The rest of the time, they operate on a run-of-river basis.

Scenario "Null Hydropeaking": The operating modes are similar to those of the "economic" scenario, but those which still causing hydropeaking are adapted in order to eliminate it completely.

Figure 1 : Système and variants studied

Hydropeaking in Heiligkreuz river section

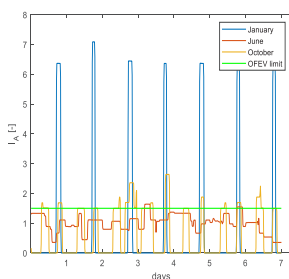


Figure 2 : I_A at the reference state

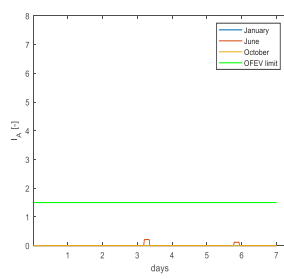


Figure 3 : I_A for both variants and all scenarios

Hydropeaking in Mörel river section

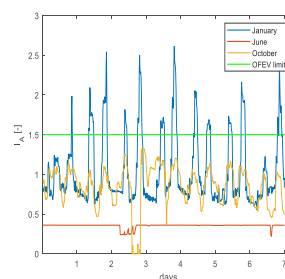


Figure 4 : I_A at the reference state

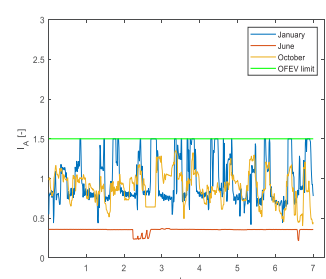


Figure 5 : I_A for the scenario null hydropeaking

Production and revenues

Table 1 : Production (ΔE [GWh/year]) and revenues (ΔR [Mio CHF/year]) differences with reference state (E_i, R_i)

Variants	Scenarios	ΔE	$\Delta E/E_i$ [%]	ΔR	$\Delta R/R_i$ [%]
Short level	BAU	10.4	2.31	0.41	2.23
	Economic	33.8	7.49	1.42	7.67
	Null Hydropeaking	23.6	5.23	0.84	4.55
Ernen Big Fall	BAU	24.4	5.39	0.94	5.07
	Economic	44.5	9.85	1.71	9.27
	Null Hydropeaking	35.2	7.80	1.19	6.46

Discussion

Variants studied allow to improve production and to mitigate hydropeaking on Heiligkreuz section but replace river section with hydropeaking by river section with residual flow. Ecological benefits induced by this replacement are not proved yet. The scenario "Null Hydropeaking" allow to delete hydropeaking on Mörel river section but cause a flexibility loss showed by a revenues reduction.

Conclusion

Based on a construction cost estimation, the short level variant appears about 6 time cheaper than the Ernen big fall variant. Solution with the smaller spatial scale and impact on the system is recommended.

References

- [1] OFEV, « Assainissement des éclusées – Planification stratégique », 2012
- [2] OFEV, « Eclusées – mesures d'assainissement », 2017
- [3] D.Tonolla, A.Bruder, S.Schweizer. (2017), *Evaluation of mitigation measures to reduce hydropeaking impacts on river ecosystems – a case study from the Swiss Alps.*

Suspended sediment in the turbine water of HPP Fieschertal in 2018

Matthias Eugster, David Felix, Robert Boes; VAW, ETH Zürich

Introduction

Sediment particles transported in the water of mountain rivers (Fig. 1) cause hydro-abrasive erosion on turbines of medium and high-head Hydro-Power Plants (HPP). This reduces the turbine efficiency and electricity production while the costs for repairs and spare parts increase.

As a basis for economic optimizations, this study aimed at quantifying the Suspended Sediment Load (SSL) in the penstock of the high-head HPP Fieschertal in the Swiss Alps throughout the year 2018.



Fig. 1: Mountain stream with proglacial lake and high suspended sediment concentration approaching the intake of HPP Fieschertal (Photo: M. Eugster, 23.05.2019)

Set-up

The HPP Fieschertal is a run-of-river scheme (Fig. 2) downstream of the Fieschergletscher which is the second longest glacier in the Alps. In the valve chamber (Fig. 3), (1) an acoustic discharge measurement installation (ADM), (2) a Coriolis Flow and Density Meter (CFDM), (3) a Laser In Situ Diffractometer (LISST) and (4) an automatic water sampler were operated to measure the suspended sediment concentration (SSC). In addition, particle size distributions between 3 and 380 μm were measured by LISST every minute.

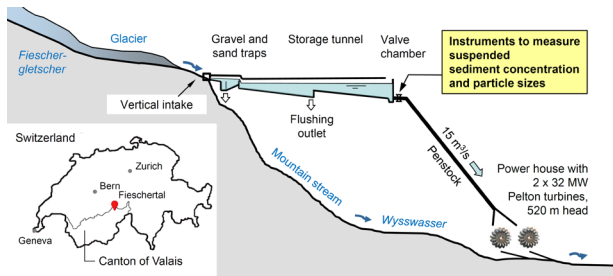


Fig. 2: Longitudinal profile of HPP Fieschertal with study site location (modified from Felix 2017)

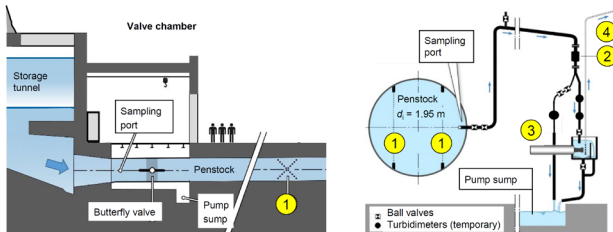


Fig. 3: Valve chamber of HPP Fieschertal with instrumentation (modified from Felix 2017)

Methods

From each water sample, the SSC was determined by weighing in the laboratory (gravimetric method). Using these reference SSC and the median particle size d_{50} obtained from LISST, the SSC were evaluated from the raw data recorded by the other instruments. The SSC from the ADM were found to be most reliable for $\text{SSC} < 0.5 \text{ g/l}$, whereas the data of the CFDM were preferred $> 1 \text{ g/l}$. Between 0.5 and 1 g/l , a weighted average of SSC from ADM and CFDM was used.

The Suspended Sediment Load (SSL) in the penstock was calculated by integrating the product of SSC and discharge over time.

Results

Suspended sediment concentration (SSC)

Suspended sediment particles were mainly transported from mid April to mid November 2018 (Fig. 4). Some SSC peaks, e.g. on June 11 (day 161), are due to rain events, but no major flood occurred in 2018. The highest SSC in the penstock was caused by a re-suspension event in the storage tunnel (Fig. 2) on August 14 (day 225): When the water level in the tunnel was drawn down while the turbines were running, the flow velocity and the bottom shear stress in the tunnel increased. This led to the transport of more and coarser particles into the penstock compared to normal operating conditions in summer when the tunnel is completely filled with water and acts a secondary trap for fine sand.

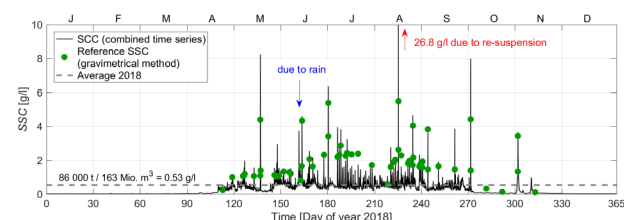


Fig. 4: Suspended sediment concentration (SSC) in the penstock of HPP Fieschertal in 2018

Suspended sediment load (SSL)

In 2018, about 86 000 t of mainly silt particles were transported through the penstock, corresponding to a specific fine-sediment yield of 0.6 mm per year in the catchment area of 58 km^2 . While the average SSC was similar to previous years, a relatively high runoff volume due to the warm summer (glacier melt) led to a rather high SSL.

In contrast to the year 2012 with a major flood event, the sediment transport rate was quite uniform during the summer months of 2018. Hence there was no need to temporarily shutdown the HPP in this year.

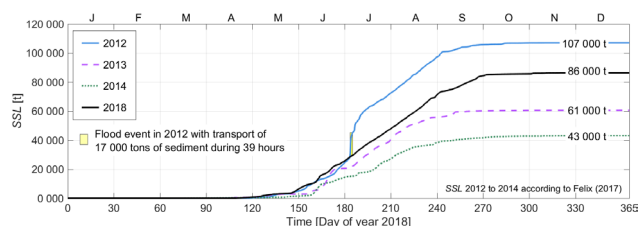


Fig. 5: Suspended sediment loads (SSL) in the penstock of HPP Fieschertal over the years

Conclusions

The SSC in the power waterway of HPPs depend not only on the weather conditions but also on the HPP operation. The annual sediment loads vary considerably mainly due to occasional flood events. Therefore, long-term data series are required to obtain reliable average values and to capture the full variability of the processes. Real-time suspended sediment monitoring serves as a basis for economic and energetic optimizations of HPP operation. Thus it contributes to the sustainable and efficient use of the hydropower potential and hence to the implementation of the Energy Strategy 2050.

References

- Abgottsporn A., Felix D., Boes R., Staubli T. (2016). Schwebstoffe, hydro-abrasiver Verschleiss und Wirkungsgradänderungen an Pelton-turbinen – Ein Forschungsprojekt am KW Fieschertal. *Wasser Energie Luft* 108(1), 9–24.
- Felix D. (2017). Experimental investigation on suspended sediment, hydro-abrasive erosion and efficiency reductions of coated Pelton turbines. VAW-Mitteilung 238 (R. M. Boes, Ed.) and Dissertation 24145, ETH Zürich, Switzerland.
- Felix D., Albayrak I., Boes R. M. (2018). In-situ investigation on real-time suspended sediment measurement techniques: Turbidimetry, acoustic attenuation, laser diffraction (LISST) and vibrating tube densimetry. *Intl. Journal of Sediment Research* 33, 3–17.

Renewal of alpine hydroelectric plants according to the spatial and temporal scales of analysis

Vincent GAERTNER, Sabine CHAMOUN¹, Pedro MANZO¹, Giovanni DE CESARE¹
¹ Hydraulic Constructions Platform (PL-LCH), EPFL

Introduction

Since the adoption of the "Energy Strategy 2050" by the Federal Council in 2017, Switzerland has been looking for new energy alternatives to the nuclear sector and ways to reduce its greenhouse gas emissions, in particular by promoting the development of renewable energies. The national hydroelectric park, which represents 59% of total energy production, has an essential place in this context of upheaval in electricity supply. In the coming years, more and more existing power plants will come to the end of the concession. In this transitional period, they must be the subject of interventions to adapt their installations and operations to future economic, energy, legislative and environmental contexts. The main objective of the project is the development of a methodology to identify and promote technical solutions to increase winter energy production and operating flexibility. It consists of a first step of diagnosing the installations reference state and then a second step of generating and analysing renewal variants. It is then applied to the case study of the Forces Motrices de Conches (GKW) and the Forces Motrices Valaisannes (FMV) power plants in Haut-Valais.

Methodology

The general methodology followed in this work consists of three main steps. First of all, the establishment of the existing system reference state aims to study the existing power plants and their environment in order to choose the spatial and temporal scales of analysis and to identify the potential for optimising operation. Renewal variants are generated according to the identified intervention possibilities. These variants are then compared using multi-criteria analysis, modelling and pre-dimensioning to produce final recommendations.

The choice of the spatial scale of analysis is intended to limit the scope of investigations for the generation of renewal variants. The approach of choice proposes to evaluate at different scales the additional potential of existing facilities and their environment in order to achieve the project objectives. If large-scale surveys are required, a simplified cost calculation of an extension of storage capacity should allow for a comparison of construction costs and potential winter production gains.

Preselection is carried out to evaluate and compare the variants using criteria on energy, technical, environmental and social aspects. Finally, a second comparison based on the results of this in-depth analysis should lead to recommendations for final solutions.

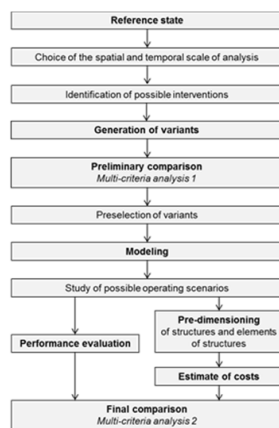


Figure 1: General approach for a hydroelectric facilities renewal project

Case study

The project applies to the Heiligkreuz (GKW), Ermen and Mörel (FMV) power plants located on the left bank of the Rhône in Haut-Valais, Switzerland.



Figure 2: Geographical location and topography of the case study region

The system has an installed capacity of 119.5 MW for an annual production of 448 GWh. Seasonal transfer of inputs is not feasible in the current state of the facilities and winter production represents between 1/10 and 1/4 of the annual production depending on the plant.

Rivers and intakes in the study area are not instrumented and the required hydrological data are only partially available. The operating data from the Heiligkreuz, Ermen and Mörel power plants and the Rhône flow measurements at Reckingen provided by the FOEN are therefore used to reconstitute the water inflow curves at the intakes.

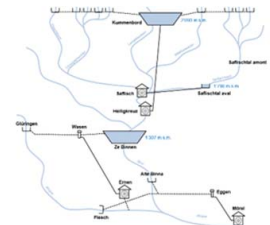


Figure 3: General scheme of the current facilities

Results

The procedure for generating adaptation concepts enables the development of 18 local variants and sub-variants based on the intervention types identified in the previous step. They can be divided into two main groups according to whether they aim to specifically optimize the use of Lentalwasser inflows or whether they propose to exploit the potential of the Safliischthal. The three of them that are preselected provide an increase in production thanks to two new power plants and seasonal storage possibilities thanks to a large capacity reservoir upstream of Kummendorf and new pumping systems between Ze Binnen and Kummendorf.

Hydraulic modelling of operating scenarios and energy performance assessment show an increase in the annual production of the three main power plants.

	Variant n°2		Variant n°4		Variant n°6	
	Scenario 1	Scenario 2	Scenario 1	Scenario 2	Scenario 1	Scenario 2
Heiligkreuz	+8.53%	+8.53%	+6.65%	+5.40%	+4.29%	+1.46%
Ermen	+6.78%	+6.71%	+6.55%	+6.47%	+6.47%	+5.82%
Mörel	+6.12%	+6.16%	+5.81%	+6.07%	+5.77%	+5.69%

Figure 4: Rate of increase in annual production from existing plants

The development of scenarios based on the seasonal transfer of inputs also provides an opportunity to rebalance the annual distribution of production by increasing winter supply.

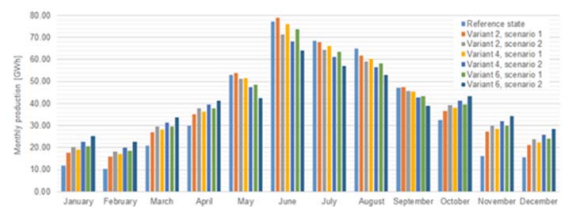


Figure 5: Monthly total production of the system in the different scenarios

The economic evaluation of the variants shows a decrease in the profitability of the largest variants due to high construction costs. A balance must therefore be found between the advantages of winter supply and the expected financial benefits.

Conclusions

The application of the methodology to a case study in Upper Valais provided different variants to achieve the objectives of increasing energy production and developing operational flexibility and seasonal storage for winter supply. It has been established that the GKW and FMV power plants in the Conches Valley have a real potential for optimization. Variants with large storage capacities have been selected and submitted for further study. Finally, modelling and pre-dimensioning steps demonstrated their relevance to the project objectives.

One of the avenues for continuing the project could be the instrumentation of strategic points of the system in order to ensure better monitoring of the available hydrological inflows and to consider optimising operation up to the limits of the current and future concession.

References

- GIOVANNI, Marco, 2017. *Rénovation d'aménagements hydroélectriques alpins*. Lausanne : Ecole Polytechnique Fédérale de Lausanne. Travail de Master.
- Guide pratique pour la réalisation de petites centrales hydrauliques. Programme d'action PACER – Energies renouvelables, Office fédéral des questions conjoncturelles, septembre 1992.
- SCHLEISS, A.J. *Aménagements Hydrauliques*. Section de Génie Civil, Laboratoire de Construction Hydrauliques, Ecole Polytechnique Fédérale de Lausanne (EPFL). Edition 2015.

Commissioning of a new fatigue test rig based on pressure oscillations

A. Gaspoz¹, N. Gonçalves¹, L. Barras¹, V. Hasmatuchi¹, C. Nicolet², S. Rey-Mermet¹

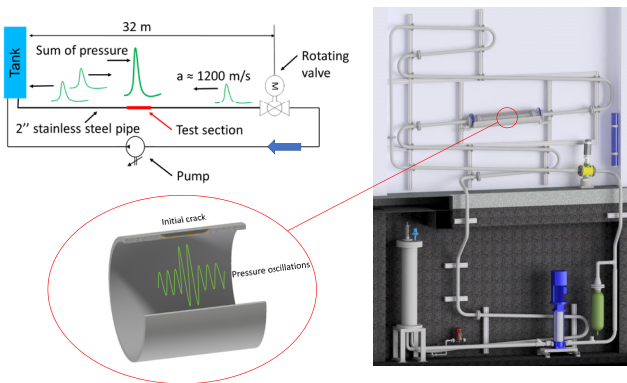
¹HES-SO Valais, School of Engineering, powder technologies and advanced materials Group, CH-1950 Sion, Switzerland, samuel.rey-mermet@hevs.ch

²Power Vision Engineering Sàrl, Chemin des Champs Courbes 1, CH-1024 Ecublens, Switzerland

Context

Hydraulic power plants are an important part of the electricity production. Most of installations have been build before the 80's. The maintenance and the research of defects are the base to ensure their security. Fatigue phenomenon appears faster when the parts contain defects.

To study the behavior of a defect under pressure oscillation, a special test rig was build in the HES-SO laboratory in Sion. The idea consists to create periodically water hammer with a rotating valve and use the resonance (sum) phenomenon in the middle of the pipe. The oscillations are comparable to those present in a penstock and responsible of a fatigue break.

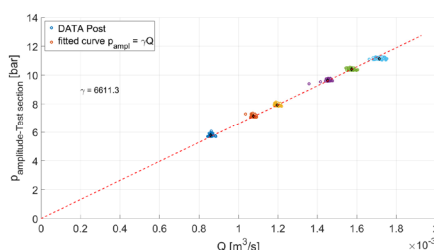
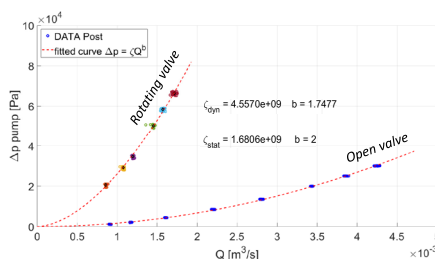


Methods

The commissioning started at the end of 2018 and the characterisation of the test rig was realized with pressure sensors during spring 2019. Numerical simulation have permit to design and chose the different operating point. Simulation were realised with the software Simsen [1] marketed by Power Vision Engineering in Ecublens, Switzerland.

Characterisation Results

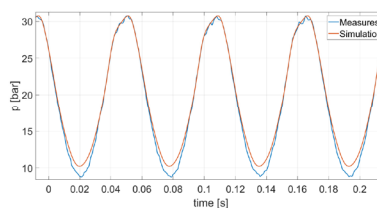
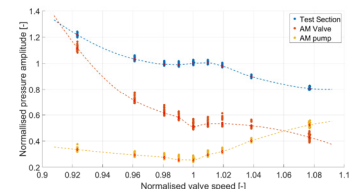
Curves of energy losses in function of the flow and the valve's position.



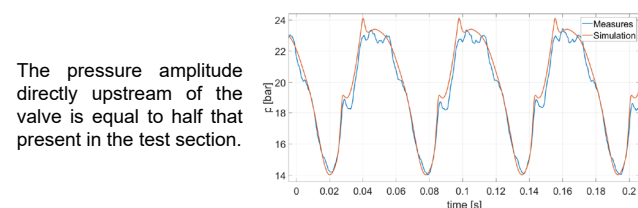
Pressure oscillation amplitude at the test section which is considerate as the half of the peak to peak difference.

Numerical Results

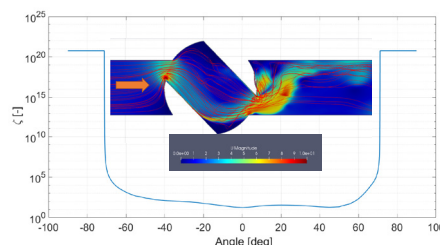
Pressure amplitude on the test section, directly upstream of the valve and the pump normalized by the values of the main operating point.



Pressure on the test section with a 88.9 x 2 mm pipe that correspond to an stress oscillation between 22 and 66 MPa.



The pressure amplitude directly upstream of the valve is equal to half that present in the test section.



The transient characteristic of the valve was simulated with the open source software OpenFOAM. The result is used in Simsen for the global transient simulation.

Conclusion

- ✓ The test rig is in function and the last corrections are planned for the end of 2019.
- ✓ The principle of cyclic water hammer in resonance was measured and corresponds to the transient simulations.
- ✓ The installation of a crack sensor has started this year. The sensor is marketed by Sensima and uses the Foucault current effect to measure the depth and the length of a crack [2]
- ✓ The first break of pipe should be realized by the end of 2019.

Acknowledgements

References

- [1] Nicolet, C., Béguin, A., Bollaert, E., Boulicaut, B., & Gros, G. (2015). Real-time simulation monitoring system for hydro plant transient surveys Int. *Journal on Hydropower & Dams*, 22(5), 62-69.
- [2] <http://www.sensimainsp.com/>

Hydraulics of Horizontal Bar Rack-Bypass Systems: Field Study at HPP Stroppel

Roland Hagenbüchli, Ismail Albayrak, Mohammadreza Maddahi, Ricardo Mendez, Robert M. Boes

Introduction

Horizontal bar rack-bypass systems (HBR-BS) are widely used for fish protection and guidance at hydropower plants (HPP). In 2014 a HBR-BS was installed at Stroppel HPP located on River Limmat in Switzerland. Axpo Power AG as the HPP operator and Aquarius [1] conducted an extensive fish monitoring campaign at this HPP in 2015 – 2017. In the present study, the hydraulics of the HBR-BS were investigated and linked to the results from the fish monitoring campaigns.

Study Site HPP Stroppel

Stroppel HPP is the most downstream power plant on the River Limmat before its confluence with the River Aare. Table 1 list the main characteristics of the HPP and its HBR-BS system.

Tab. 1: Main characteristics of Stroppel HPP and its HBR-BS

HPP Stroppel		HBR-BS			
Design discharge	[m³/s]	33	Bar opening	[mm]	20
Installed power	[kW]	840	Length of the rack	[m]	25.3
Installed turbines	1 Francis, 2 Kaplan		Horizontal rack angle	[°]	38
Fish region	Grayling and Barbel		Discharge in the bypass	[m³/s]	0.69

During the fish monitoring campaign, 28 fish species were detected. 86% of the fish had a body length < 10 cm and 98% of them were smaller than 20 cm. Moreover, the monitoring results indicated that the HBR-BS performed well independent of fish size and species and the delay in downstream migration was short. However, some small fishes < 10 cm were observed behind the rack using an ARIS sonar system (1.6 to 3.2% of the small fishes that migrated via bypass), whereas fish with a body length larger than 10 cm were not detected behind the rack. Furthermore, no fish impingement on the rack was observed during the monitoring.

Methods

An Acoustic Doppler Current Profiler (ADCP) mounted on a remote controlled boat with RTK-GPS was used to investigate the hydraulics of the HBR-BS (Fig. 1). Velocity measurements were conducted in 13 cross-sections normal to the flow direction in the headrace channel and in two sections parallel to the rack (Fig. 2). In addition, six stationary measurements were conducted at selected positions as shown with red crosses in Fig. 2.

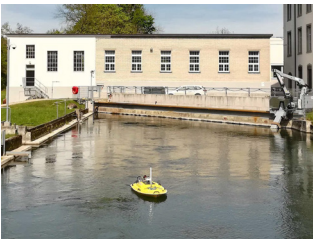


Fig. 1: Measurement device in the headrace channel of HPP Stroppel.

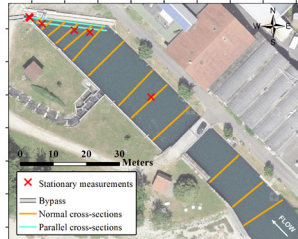


Fig. 2: Positions of velocity measurements (orthophoto [2])

Results and Discussion

Figure 3 shows the depth-averaged velocity magnitudes along the headrace channel. The vectors indicate longitudinal and transverse velocity directions. The velocity field shows that the main flow has the tendency to shift towards the left side, where the bypass entrance is located. Furthermore, due to the low ratio of channel width to flow depth ≈ 4 , the flow is 3D and the maximum velocities are concentrated at the channel center and below the water surface (Figs. 3 and 4).

Figure 4a shows the distribution of the velocity component normal to the rack (v_n) in a cross-section along the rack measured at 1.7 m upstream of the rack. $y = 0$ indicates the left bank of the channel. Close to the surface at the centre of the rack, the flow velocities exceed the general design criteria of 0.5 m/s [3] with the maximum value of 0.7 m/s.

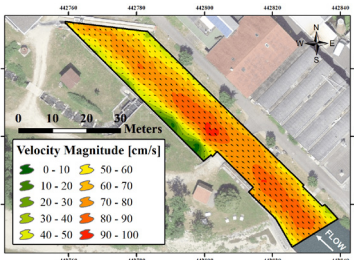


Fig. 3: Depth-averaged velocity magnitude along the headrace channel of HPP Stroppel (orthophoto [2]).

Fig. 4b shows the ratio of the rack-parallel (v_p) to the normal (v_n) velocity components. A ratio of $v_p/v_n > 1$ is recommended in order to guide approaching fish towards the bypass [3, 4]. From the center to the left channel side, where the bypass entrance is located, the ratio is uninterruptedly higher than 1 and therefore indicating a well-guiding flow field.

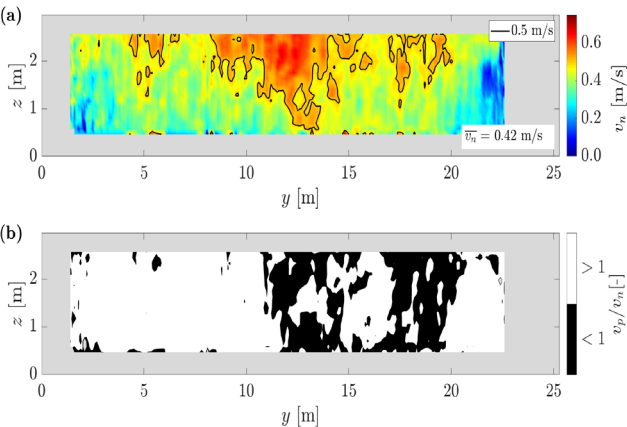


Fig. 4: Cross-sectional distributions of the velocity normal to the rack (v_n) (a) and the ratio of the rack-parallel to the rack-normal velocities (v_p/v_n) (b).

Conclusion

The hydraulics of HBR-BS at Stroppel HPP were investigated. The results show that the HBR-BS creates favorable flow conditions for fish protection and guidance at a large portion of the rack area and up to the bypass. Even though small fish with a body length < 10 cm could physically pass the rack, only a small fraction of them was observed behind the rack. Such results indicate that the rack and bypass are well designed and positioned. Overall, Stroppel HPP is a promising example of a good implementation of a HBR-BS for protection and guidance of downstream migrating fish and hence the restoration of the longitudinal connectivity in riverine systems.

References

[1] Zaugg, C. and Mendez, R. (2018). Kleinwasserkraftwerk Stroppel - Wirkungskontrolle Fischabstieg am Horizontalrechen mit Bypass. Axpo Kleinwasserkraft AG.
[2] map.geo.admin.ch (2019). Kartenserver der Schweiz.
[3] Courret, D. and Larinier, M. (2008). Guide pour la conception de prise d'eau ichtyocompatibles pour les petites centrales hydroélectriques.
[4] Raynal, S., Chatellier, L., Courret, D., Larinier, M., and David, L. (2013). An experimental study on fish-friendly trashracks – part 2. angled trashracks. *Journal of Hydraulic Research*, 51(1): 67–75.

Two-phase flow hydraulics of low-level outlets

Benjamin Hohermuth, Lukas Schmocker, Robert Boes – VAW, ETHZ

Introduction

Low-level outlets are key safety elements of high-head reservoir dams. The load on low-level outlets will likely increase in the near future due to more frequent sediment flushing and dam heightening. Therefore, an improved understanding of their hydraulic properties is necessary. A common outlet configuration uses a high-pressure vertical slide gate discharging into a free-flow tunnel. The high-speed water jet in the outlet tunnel leads to considerable air entrainment and transport resulting in negative air pressures, which can aggravate problems with gate vibration, cavitation, and slug flow. Sufficient air supply via an air vent mitigates such problems. However, current methods for estimating the required air demand do not incorporate all factors affecting design of air vents for low-level outlets. Additionally, information on two-phase flow hydraulics regarding e.g. flow pattern or mixture flow depth is almost inexistent.

The hydraulics of low-level outlets were investigated in a doctoral thesis using hydraulic model tests, prototype measurements and numerical simulations. The main findings are summarized herein.

Results

Air-water flow pattern

Four different air-water flow pattern were observed in the model and prototype tests:

- Spray flow; for relative gate openings ≤ 0.12 and contraction Froude numbers $F_c \geq 40$
- Free-surface flow; significant shockwave formation due to detachment of corner vortices was observed for $0.3 \leq$ relative gate opening ≤ 0.7 (Fig. 1a).
- Slug flow; strong counter-current air flow can trigger the formation of slugs. A novel flow pattern map allows to identify and consequently avoid slug flow (Fig. 1b).
- Pressurized flow; for relative tunnel fillings ≥ 0.8 the downstream tunnel end was pressurized.

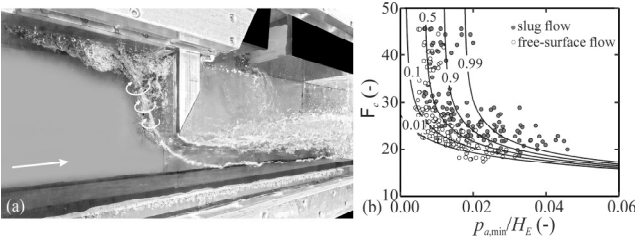


Figure 1: (a) gate vortices observed in model tests; pressurized air added for visualization. (b) Flow pattern map to identify slug flow; lines denote different probabilities of slug formation. H_E =energy head at gate, $p_{a,min}$ =minimum air pressure in gate chamber.

Air demand

The influence of air vent, tunnel length L_t and tunnel slope S_t on the relative air demand β of low-level outlets was studied in extensive model tests. The air demand is primarily a function of F_c and the air vent properties. Increasing L_t leads to an increase in air demand, the effect of S_t is small. Prototype measurements were used to validate and extend the model-based results leading to a new predictive equation:

$$\beta = \frac{Q_{a,o}}{Q_w} = 0.08 F_c^{1.3} \left(\frac{A_v}{A_t (\zeta + 1)^{0.5}} \right)^{0.8} \left(\frac{L_t}{h_t} \right)^{0.25} \quad (1)$$

where A_t =tunnel area, A_v =air vent area, h_t =tunnel height, $Q_{a,o}$ =air discharge through air vent, Q_w =water discharge, ζ =air vent loss coefficient.

Equation 1 captures the available prototype data roughly within $\pm 50\%$, thus considerably improving air demand predictions compared to order of magnitude errors of existing approaches.

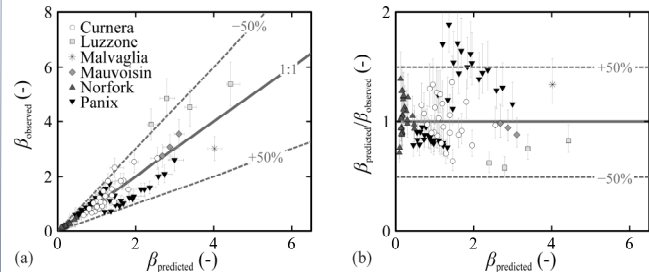


Figure 2: Comparison of (a) observed prototype air demand versus predicted β (Eq. 1). (b) relative error versus predicted β .

Hydraulics air-water flow

High velocities of up to 22 m/s in model tests allowed to gather data at prototype like conditions leading to the following results:

- Void fraction c ; the void fraction profile can be described by an advection-diffusion equation (Fig. 3a). The mean void fraction C_m reaches a maximum after the gate and decreases from thereon.
- Interfacial velocity u ; a wall-jet like profile was observed close to the gate, whereas a velocity-dip profile occurred further downstream. The latter can be described with a novel modified power law (Fig. 3b).
- Mixture flow depth h_{90} ; the development of h_{90} can be described with a novel empirical approach based on a simplified backwater calculation (Fig. 3c).

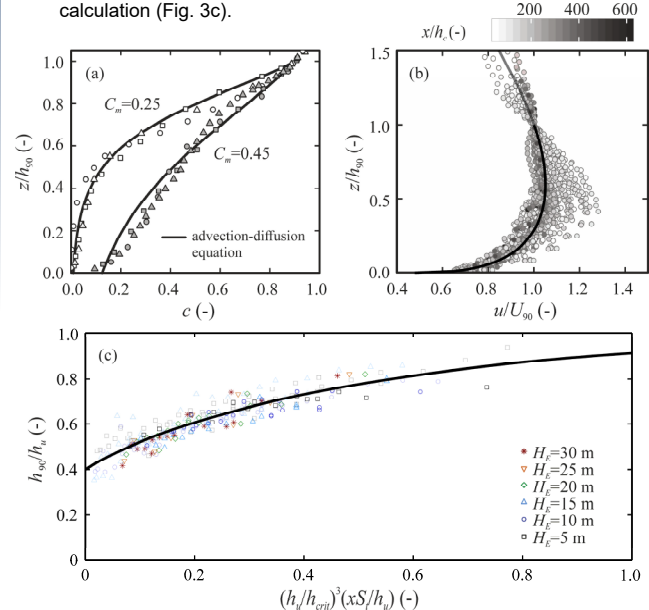


Figure 3: (a) c -profile for different C_m . (b) u -profile at different dimensionless distances, h_c =contraction flow depth. (c) Simplified backwater curve h_{90} , h_{crit} =critical flow depth, h_u =uniform (non-aerated) flow depth, S_t =tunnel slope.

Conclusions

A detailed model study on air-water flows in low-level outlets was conducted. The results were complemented by prototype measurements. The findings presented herein allow for an improved design of low-level outlets for future infrastructure adaptations.

Acknowledgement

This project is financed by the SNF Grant No. 163415 and is embedded in the SCCER-SoE framework. The prototype tests were financially supported by the Lombardi Engineering Foundation and conducted in cooperation with Ofible.

Numerical investigation of HPP layouts and their effects on fish guidance racks

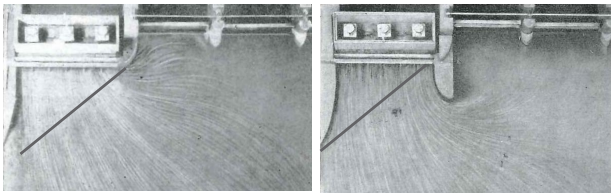
Andreas Huwiler

Introduction

Hydro power plants (HPP) inhibit downstream fish migration. Fish guidance structures (FGS) can be used to improve this situation. The goal of this study was to analyze the upstream flow fields at different HPP layouts. The analyses were conducted with computational fluid dynamics (CFD). The effect of different measures at the HPP layouts to fish guidance structures were investigated.

Background

There are different concepts to ensure downstream fish migration. One criterion for good fish guidance efficiency is the ratio between the velocity parallel (v_p) and the velocity normal to the rack (v_n). This ratio (R_v) should be higher than one [1]. In this study, horizontal bar racks (HBR) were investigated since HBRs have little influence on the flow field. Different physical studies were conducted at the VAW to investigate HBR [2]. At HBRs, the ratio depends mostly on the HPP layout. The layout influences the approach flow to the turbines and to the rack, as can be seen in figure 1. The pillar at the bay unit HPP layout (1b) improves the ratio in front of the rack.



a): without pillar b): with pillar
Fig. 1: Flow field at a bay unit HPP [3]. The rack is simplified as a line.

Methodology

Using CAD Software a block unit HPP, a bay unit HPP and a HPP with side intake were built (fig. 2). Based on this layouts different simulations were conducted with the CFD Software FLOW-3D. The HBR was substituted as a baffle. The analysis of the approach flow of the rack was of particular interest. Furthermore, the influence of different discharges over the weir and different angles of the rack to the fish guidance were examined.

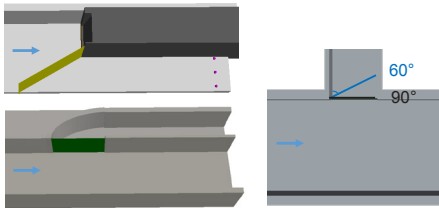


Fig. 2: The three investigated geometries: a block unit HPP, a bay unit HPP and a HPP with a side intake.

For the block unit HPP layout, observed data was available from a physical model of the VAW laboratory. With this data, the results of the simulation could be validated. The settings of the validated simulation could be used to test the other two layouts for which no laboratory analyses were carried out. The steps are shown in the scheme in figure 3.



Fig. 3: Schema of the conducted work

Results and Discussion

The flow field was analyzed with horizontal planes of the flow velocity in x-direction (U) and different cross sections (CS). The most important CS was the one along the rack where the R_v was plotted. Figures 4 and 5 of the simulated and measured results of the block unit HPP are shown as examples. The simulated data represents the measured data in a high agreement. Differences in the horizontal flow field are direct in front of the weir and after the rack. At the CS along the rack, the biggest differences can be identified direct at the weir on the left side of the plot. The plot illustrates how the fish guidance worsens along the rack towards the weir ($R_v < 1$).

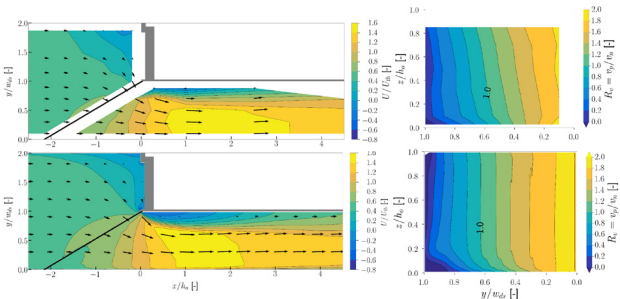


Fig. 4: Horizontal plane at $z=0.5h_0$ of U/U_m Fig. 5: Cross Section of R_v along rack

In figure 6, the cross sections of the HPP with side intake are shown. In the two pictures, R_v is shown at different rack angles.

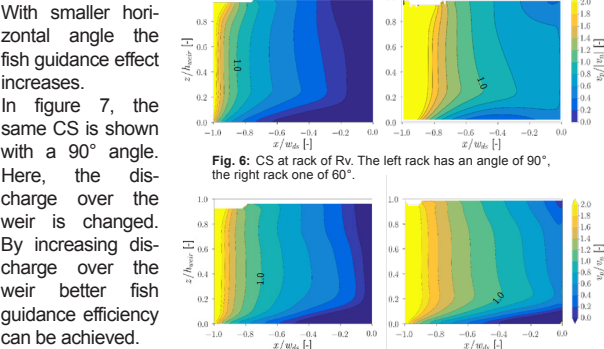


Fig. 6: CS at rack of R_v . The left rack has an angle of 90°, the right rack one of 60°. Fig. 7: CS at rack of R_v . On the left, the weir discharge is 40% of Q_{in} and 60% on the right.

Conclusion

The results of different CFD simulations at a block unit HPP could be verified with measurements from a physical model. Thus, the HBR could be well implemented as a baffle in FLOW-3D. Additional HPP layouts were analyzed. There, the influence of different rack angles and discharges on the FGS could be quantified. Both measures can be used to improve the R_v . Which measure should be implemented depends on the studied layout and existing restrictions. Because this works includes an approach how a HBR can be implemented in CFD studies, the head loss caused by the rack can be included in the evaluation.

References

[1] U.S. Department of Interior Bureau of Reclamation (USBR) (2006). Fish protection at water diversions: a guide for planning and designing fish exclusion facilities. Denver, CO: USBR.
[2] Meister, J., Fuchs, H., Albayrak, I., Boes, R.M. (2018). Horizontal bar rack bypass systems for fish downstream migration: state of knowledge, limitations and gaps. In Proc. 12th International Symposium on Ecohydraulics, Tokyo, Japan.
[3] Mosonyi, E. (1987). Water Power Development, volume one: Low-head power plants. Akadémiai Kiadó, Budapest.

Run-up of Impulse Wave Trains

Maximilian Kastinger, Frederic Evers, Robert Boes

Introduction

Very rapid gravity-driven mass movements including landslides, rock-falls, avalanches and glacier calvings can cause large water waves in open oceans, bays, natural lakes and reservoirs. Resulting impulse wave trains propagate away from the impact location and can run up several meters high on the shore. Possible consequences are damages to settlements and infrastructure or overtopping of dams, as shown by numerous historic events in Switzerland and abroad. Reservoirs are of particular interest, as there is usually a freeboard of just a few meters between the still water level and the dam crest.

While the run-up of single and periodic waves has already been extensively researched, there is only few knowledge about the multiple run-up of irregular wave trains. Therefore, the aim of this master's thesis was to investigate the run-up behavior of impulse wave trains and to develop an approach in order to estimate their run-up heights.

Methodology

Physical model tests were carried out in a 2D wave channel. The waves were generated by mesh-packed granular material sliding into the water body. First, the unconfined wave propagation was measured with ultrasonic distance sensors (UDSs). Then, the experiments were repeated with a barrier of different slope angles β , which was installed at the location of one of the sensors. The run-up was recorded with cameras. Fig. 1 shows the test setups for unconfined and run-up experiments.

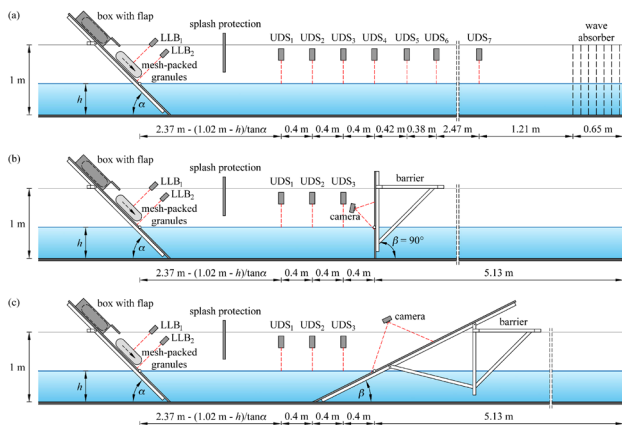


Fig. 1: Test setup for (a) unconfined wave propagation, (b) wave run-up at a vertical barrier and (c) wave run-up at an inclined barrier, exemplarily being installed at the location of UDS₄

Different wave characteristics were achieved by varying the water depth h , slide angle α , impact velocity V_s , sliding mass m_s and grain density ρ_g . Target wave properties include the wave crest and trough amplitudes a_{ci} and a_{ci} , respectively, wave heights H_i , wave celerities c_i , wave periods T_i and wave lengths L_i . The wave run-up R_i refers to the still water table, as shown in Fig. 2.

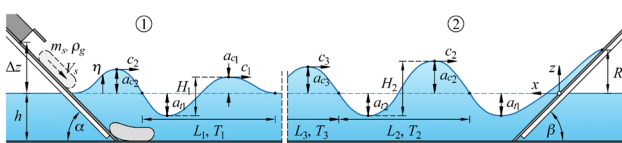


Fig. 2: Definition scheme with the governing parameters for ① wave generation and ② wave run-up

Results and Discussion

Breaker types

A different run-up behavior of the waves was observed. It was divided into non-breaking (NO), surging breaker (SU) and plunging breaker (PL). Fig. 3 illustrates these three types for an exemplary experiment.

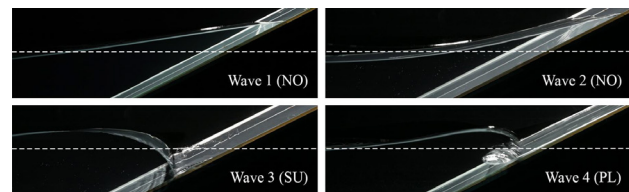


Fig. 3: Run-up behavior of the first four waves for a barrier slope angle $\beta = 26.6^\circ$, the first two waves are non-breaking (NO), the third wave is a surging breaker (SU) and the fourth wave is a plunging breaker (PL)

As the breaker type influences the run-up height significantly, a prediction criterion based on the surf similarity parameter $\xi_i = \tan \beta (H_i/L_i)^{1/2}$ (Iribarren and Nogales, 1949) and the relative wave height H_i/h is proposed (Fig. 4).

Non-breaking waves (NO):

$$\xi_i > 2.1 \left(\frac{H_i}{h} \right)^{-0.15} \quad (1)$$

Surging breakers (SU):

$$1.5 \left(\frac{H_i}{h} \right)^{-0.15} \leq \xi_i \leq 2.1 \left(\frac{H_i}{h} \right)^{-0.15}$$

Plunging breakers (PL):

$$\xi_i < 1.5 \left(\frac{H_i}{h} \right)^{-0.15} \quad (2)$$

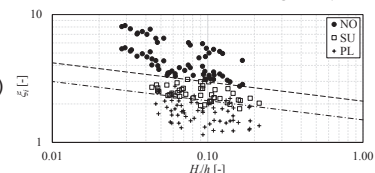


Fig. 4: Surf similarity parameter ξ_i versus relative wave height H_i/h for the different breaker types and the proposed criteria (--- Eq. (1) and (---) Eq. (2))

Run-up heights

A new prediction equation for the run-up heights is proposed (Eq. (3)). Fig. 5 shows the measured over predicted run-up heights. While non-breaking waves and surging breakers are represented well, plunging breakers are overestimated.

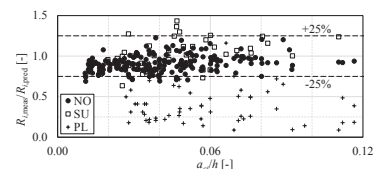


Fig. 5: Measured over predicted (Eq. (3)) run-up height $R_{i,meas}/R_{i,pred}$ versus relative wave crest amplitude a_{ci}/h

$$\frac{R_i}{h} = 2 \frac{a_{ci}}{h} e^{\frac{0.4 a_{ci}}{h}} \left(\frac{c_i}{\sqrt{gh}} \right)^{-0.25} \left(\frac{90^\circ}{\beta} \right)^{0.2} \left(\frac{a_{ci}}{H_i} \right)^{-0.45} \left(\frac{a_{ci}}{\sqrt{gh}} \right)^{-1.25} \quad (3)$$

Conclusion

A new data set with run-up heights of impulse wave trains for later reuse was created. Based on this, a new breaker type criterion and run-up prediction equation are proposed. Tests with additional barrier slope angles and further data analysis are required in order to develop a well founded, practicable run-up equation for impulse wave trains.

References

Iribarren, C. R., Nogales, C., 1949. "Protection des ports (Harbour protection)". 17th International Navigation Congress, Lisbon, Section 2, Communication 4, 31-80. (In French)

Assessing the acceptability of concrete dam submergence considering scour

Labrosse L., Chamoun S. and Manso P. A.

Plateforme de Constructions Hydrauliques, Ecole Polytechnique Fédérale de Lausanne,
labrosse.lucas@gmail.com sabine.chamoun@epfl.ch pedro.manso@epfl.ch

Why ?

For many dam operators, their assets are aging in a context that evolves both with new flood assessment methods and new legal or normative frameworks. Building new outlet structures to ensure enough flood release capacity can be expensive and limited. Figure 1 presents the reason for submergence acceptability assessment for a generic case, based on a real dam [1].

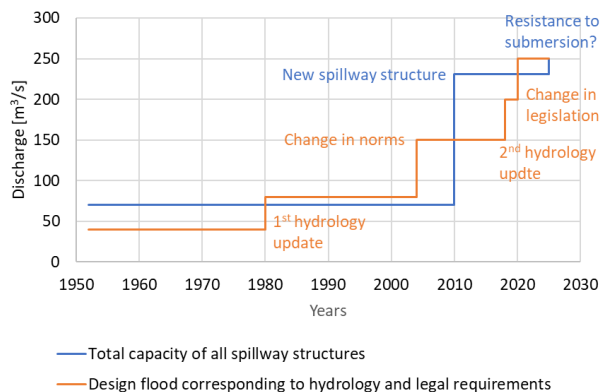


Fig. 1 Hypothetic dam history regarding flood release capacity

Submergence can be an alternative, but the dam stability has to be guaranteed and therefore it raises a few questions:

- Can the dam withstand higher reservoir levels above the crest?
- Which flood events can be accepted?
- What is the acceptable residual risk?
- To which extent is dam toe scour acceptable, considering the dam's or the abutment's instability?

This last question can be the most challenging one.

The proposed method

Divided in four modules, the method offers a framework to consider the different inputs necessary to assess the risk of dam instability due to scour following dam submergence (Fig. 2), due to insufficient conventional spilling capacity. The vulnerability to scour formation is assessed based on the duration of the submergence events, on the geometry of the falling nappes, on the downstream tailwater levels and on dam foundation & riverbed rock conditions. Then, scour evolution is assessed through different methods, considering to some extent the complexity of the processes taking place during scour progress by the interaction of air, water and rock.

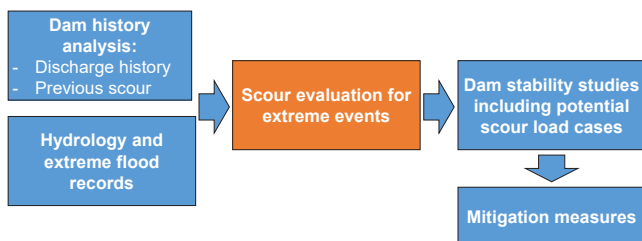


Fig. 2 Simplified chart of the proposed method for risk assessment

One of the most challenging issues in rock scour assessment is to account for the effect of time [1]. **Ultimate scour methods (USM)** allow estimating scour extent for a given discharge assuming it last long enough to reach an equilibrium configuration. **Energy-based methods (EBM)** [7,8] focus on scour progress as function of a chronological sequence of spillage discharges, varying in intensity and duration.

EPFL's **Comprehensive Scour Model (CSM)** [1] illustrates a possible way to sequentially link several physical processes, one of them being time-dependent. Rock fracture propagation under hydrodynamic loads is modelled using the Paris-Erdogan fatigue law and hydrodynamic loads defined according [2,3,4,6]. Recently, a novel EBM model was proposed by [5] considering only the **Excess Energy (EEBM)** available for scour at each given moment. The four previous methods allow having multiple truncated entries to inform decisions and risk assessment. Figure 3 graphically shows the required data to properly calibrate such methods.

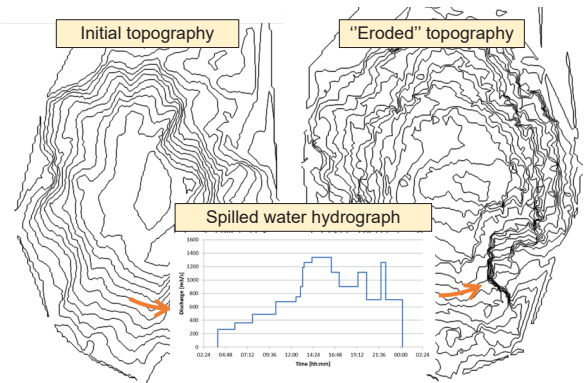


Fig. 3 Calibrating scour computation with passed spill events

Results

The general method was applied to two different dams. The first one is a dam located at a high altitudes with a fairly small reservoir and ungated crest overflow spillway. A Piano Key Weir spillway was added recently to ensure enough capacity for the revised millennial flood. The second dam is quite different, situated at intermediate altitudes and equipped with a three-bay gated spillway with ski-jumps for a total capacity of 5800 m³/s. The study of the first dam revealed that no scour had occurred yet in over 50 years. The scour analysis with USM methods showed that some erosion could occur for extreme flood events with a return period of 5000 years or more. However, the EEBM time-accounting method [5], based on the potentially available energy for scour, showed that the flood event duration was too short for any serious erosion to occur. For the second case study, with gated spillways, the available plunge pool bathymetries and spillage records allowed obtained site constants of scour progression (according [8]) and estimating scour from extreme events. The application of the EEBM showed interesting results as well, indicating that instead of using site constants to calibrate Spurr's scour evolution function, one should rather use event-related constant for calibration of such function (i.e. the same event might not produce the same scour increase if occurring at different chronological moments in the spillage records).

Further application of these methods could help to better assess how rock quality, discharge intensity and duration are linked to the equilibrium state of a scour pool. Indeed, better knowledge of possible scour evolution can help with assessing the acceptability of dam submergence.

References

- [1] Blancher, B., Laugier, F., & Leturco, T. (2015). Méthodes d'évaluation du risque d'érodabilité des fondations soumises à déversement. Colloque CFBR, Chambéry.
- [2] Bollaert, E., & Schleiss, A. (2005). Physically based model for evaluation of rock scour due to high-velocity jet impact. *Journal of Hydraulic Engineering*, 131(3).
- [3] Duarte, R., Pinheiro, A., & Schleiss, A. (2016). An enhanced physically based scour model for considering jet air entrainment. *Engineering*, 2, pp. 294-301.
- [4] Federspiel, M. (2011). Response of an embedded block impacted by high-velocity. Thèse de doctorat, EPFL, Lausanne.
- [5] Labrosse L. (2019) Résistance ultime au déversement des barrages en béton, EPFL Master thesis (Supervisors: Manso, Chamoun, De Cesare).
- [6] Manso, P., Bollaert, E., & Schleiss, A. (2009). Influence of plunge pool geometry on high-velocity jet impact pressures and pressure propagation inside fissured rock media. *ASCE J. Hydraulic Engineering*, 135(10):783-792.
- [7] Manso, P., Marques, M., Almeida, F., Canellas, A., & Botelho, M. (2007). Rock scour downstream ski-jumps : comparison of prototype observations with analytical and physical-model estimates. 32nd IAHR Congress, Venice.
- [8] Spurr, K. (1985). Energy approach to estimating scour downstream of a large dam. *Water Power and Dam Construction*, 37(11).

Solving of a Lifting Problem in a Pumped Storage Power Plant

Daniel Pace, Giovanni De Cesare, Pedro Manso, Kaspar Vereide, Livia Pitorac, Leif Lia

Email: daniel.pace@alumni.epfl.ch

Motivation

The construction and upgrading of pumped storage hydropower plants (PSHP) will be very beneficial in the years to come in order to regulate the power systems. They are very flexible and allow covering peak demands and storing energy on a large scale.

In this work, the Duge PSHP in Norway is used as a case study. The power plant has two Francis reversible pump-turbines (RPT) with a total installed capacity of 200 MW. In 2017, however, the turbines were refurbished and since then, a lifting problem occurs at the rotor of one of the turbines (Unit 1) when generating at a high load. As a consequence of this problem, the generation has to be restricted to 80% of the maximal load, i.e. 160 MW. The aim of this work is to understand the causes of the lifting and to find a civil engineering solution to this problem by modifying the waterway of the power plant.



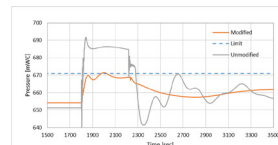
Trash rack in the Duge power plant

Results

In order to solve the lifting problem, three solutions have been selected. The first aims to avoid any problems in the worst load case and to be able to run the power plant at 200 MW again. The second aims to avoid any problems in a normal load case and to run at 200 MW as well. Finally, the third solution aims to be lighter on a technical and economic point of view and to be able to run the power plant at 185 MW. For each solution, the downstream pressure is compared to the unmodified power plant.

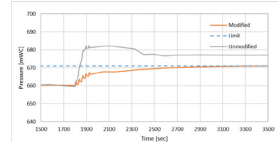
Solution 1

- Addition of a downstream air cushion surge tank
- Addition of a 6 km parallel tunnel in the tailrace



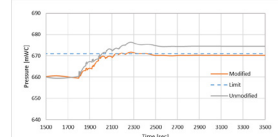
Solution 2

- Increase of volume in the surge tank upper chamber
- Addition of a 6 km parallel tunnel in the tailrace



Solution 3

- Addition of a 6 km parallel tunnel with smaller section in the tailrace

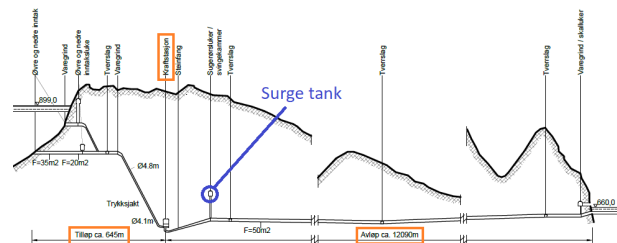


After an economic analysis is made, the final costs for each solution are estimated considering the construction works (new access tunnels, excavation, draining of tailrace tunnel, etc.) and the losses due to the power plant outage. The costs are given in different currencies (1 NOK = 0.1177 CHF and 1 NOK = 0.1008 EUR):

	Solution 1	Solution 2	Solution 3
Norwegian kroner [NOK]	275 million	215 million	162 million
Euros [EUR]	27.7 million	21.7 million	16.3 million
Swiss francs [CHF]	32.3 million	25.3 million	19.0 million

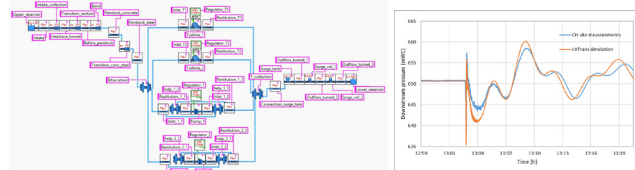
Methods and materials

The Duge PSHP has a very long tailrace tunnel (12 km) in comparison to the headrace tunnel (650 m). The high friction losses due to the long tailrace give a high downstream pressure rise at the RPT units in generating mode.



Duge power plant layout

In order to propose modifications of the power plant, a model is made on LVTrans, a numerical modelling freeware allowing to calculate transients in a loaded pipe system [1]. To simulate the real behaviour of the prototype, the model is calibrated against downstream pressure measurements, done at the draft tube wall for a turbine shutdown.



LVTrans model of the Duge power plant (left) and calibration (right)

The calibration is considered satisfactory, since only the first pressure peaks, which are the worst, are of interest for the lifting problem. The lifting of the rotor (246 tons) at Unit 1 occurs when the resulting vertical force acting on the runner is directed upwards; the downstream pressure is therefore the significant factor to consider. Norconsult, a Norwegian consulting company, calculated that 1 [mWC] downstream pressure change = 4.1 [tons] of lifting force. This is obtained by multiplying the pressure by the surface of the outlet. Moreover, the maximal lifting force acting on the runner should be no more than 75 tons [2]. Considering this, it is possible to have a threshold that the downstream pressure should not exceed in order to safely run the power plant without the lifting problem.

Discussion

As showed in the results, the modifications of the power plant improve both the steady and unsteady states and allow the downstream pressure at Unit 1 to remain under the critical threshold. However, the solutions seem to be disproportionate, considering the total amount of the required investments and construction works. A limitation of the economic analysis is that only the total costs are considered, but not the associated benefits of having more power available.

Finally, the Duge power plant will receive new runners in the future, which means that the problem may be solved in a few years. Considering all these conclusions, it seems that it is probably better to not opt for a civil engineering solution to solve this lifting problem.

References

- [1] Svingen, B., 2016. *LVTrans manual*. Sintef & NTNU, Trondheim
- [2] Norconsult, 2014. *Aksjalkrefter - måleresultater og gjennomgang av tiltak*. Sira Kvina Power Company, restricted access

Renewal of the Ritom hydropower plant

Jakob Siedersleben, Samuel Vorlet, Giovanni De Cesare, (Nicola Tatti, Urs Müller, Graziano Sangalli)

Context

On the basis of the Water Protection Act of 2013, a new generation of regulating reservoirs is under construction across Switzerland. It requires that all Swiss operators of hydroelectric power plants must eliminate within 20 years all severe issues caused by the rapid change of water discharge, called hydropeaking, due to the exploitation of hydrodynamic power. In Tessin, the hydroelectric power plant constructed in 1921 will be modernized. In the framework of this modernisation a new powerhouse with three machine groups will be constructed. In order to minimize the effects of hydropeaking, a regulating reservoir with a volume of 100.000 m³ is planned. The discharge exiting the reservoir can be controlled by a regulating structure which leads the water via an outlet in the Ticino. Due to the new reservoir, the course of the river Foss has to be changed and four sills will be installed. Fig. 1 shows the current and the planned situation.

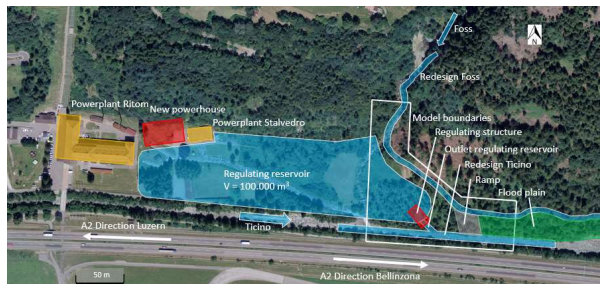


Fig. 1: Scheme of the modeled area

Objectives

The Laboratory of Hydraulic Constructions of the EPFL was mandated to execute experiments on a physical model. The following objectives were determined for the project:

- Concept validation of the planned geometry of the Ticino, the regulating reservoir and the Foss
- The investigation of the influence of the regulating structure on the Ticino
- The behaviour of the whole system under flooding up to an EHQ (extreme flood)
- The analysis of floating debris and debris flow in the Ticino and the Foss

Physical Modelling

The modelled area is 215.2 m long in flow direction of the Ticino and 181.2 m wide perpendicular to the flow direction. The modelled area is illustrated in Fig. 1. The model was constructed with a scale of 1:40 according to the Froude similitude.

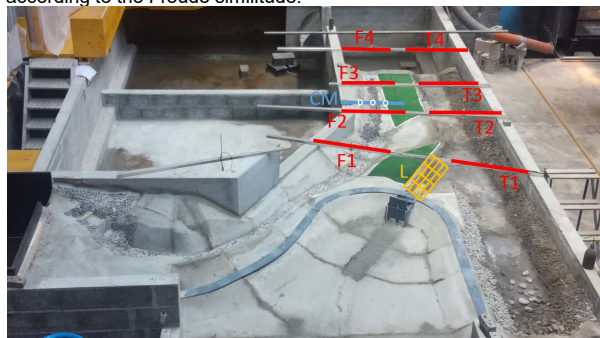


Fig. 2: The model and the eight ultrasound sensors (red), three current meter locations (blue) and the twenty-five laser locations (yellow)

In order to analyse the model, the water heights are measured at eight locations with ultrasound sensors. The height of the riverbed is measured with a red laser on a grid of twenty-five points. The flow velocities are measured with a current meter at three points. The physical model and the measuring positions are illustrated in Fig. 2. Furthermore, visual observation and colorant was used to determine dead and recirculation zones and determine possible locations prone for deposition of sediments.

Results

The tests showed a well-functioning of the whole system. But the course of the Foss had to be adapted. Furthermore, rock sills were installed and the roughness of the riverbed was increased. With these adaptations the desired maximum capacity of $Q_{\text{Foss}} = 60 \text{ m}^3/\text{s}$ is exceeded. Dependent on the discharge combination of the Ticino and the outlet of the regulating structure, one must expect sediment accumulation either at the outlet of the regulating reservoir or at the embouchure. Furthermore, one must expect a scour hole dependent on the discharge at the outlet of the regulating reservoir and the discharge of the Ticino as illustrated in Fig. 3. However, the main influence on the depth of the scour hole is the discharge in the outlet of the reservoir.

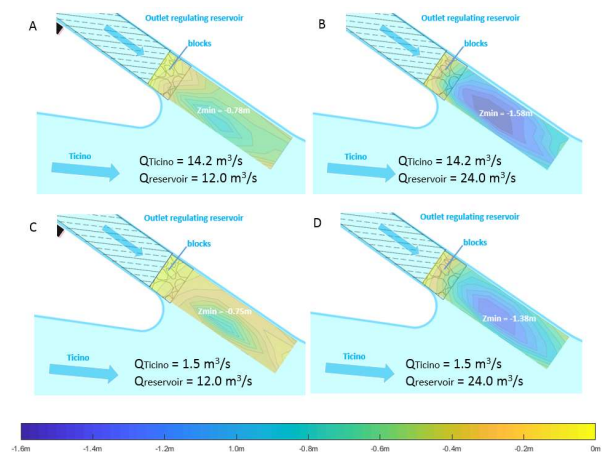


Fig. 3: The scour hole depth after the outlet of the regulating reservoir

The investigation of the floods showed that the Foss will overflow in the regulating reservoir. The regulating reservoir will overflow over the southern bank in the Ticino and the Ticino will overflow at an HQ100 over the southern bank in direction of the high way. Although the Foss overflows already significantly earlier, it inundates only the flood plain and the ramp, which does not pose any problems.

The experiments with debris flow in the Foss show that it will be transported until the ramp were it accumulates. However, if the discharge of the Foss is sufficient enough, the debris flow can overflow in the regulating reservoir as well. On the other hand, floating debris did not pose any problems in the Foss, on the contrary to the Ticino, where there can be accumulations at the outlet of the reservoir observed.

References

- Bassin de démodulation des rejets d'une centrale hydroélectrique : Barrage de Ritom ; Cédric Egolf ; 2019
- Erneuerung des Wasserkraftwerkes Ritom; Hydraulische Modellversuche; LCH Offerte 11/2017; 31.08.2017
- Auslaufbauwerk Demodulationsbecken – Verlegung Fossbach – Pflichtenheft für physikalische Modellversuche; Ritom SA (Bauherr); 02.08.2017
- Wasserkraftanlage Ritom; 28.06.2019; Retrieved from <https://www.aet.ch/DE/Impianto-idroelettrico-del-Ritom-ba89fd00#.XRZXFuszZaQ>

Hydro-abrasion at hydraulic structures

Damiano Vicari, Dila Demiral, Ismail Albayrak, Robert M. Boes
 ETH Zurich, Switzerland

Motivation and objectives

Sediment transport from glacier basins, rivers and waterways have strongly increased under the effect of climate change. As a consequence, high sediment transport rates combined with high flow velocities cause severe hydro-abrasion at hydraulic structures such as Sediment Bypass Tunnels (SBTs) and bedrock incision in high-gradient mountainous streams. A better understanding of the physical processes of turbulent flow characteristics, bedload particle motion, and hydro-abrasion and their interrelations is of prime importance for both sustainable use of hydraulic structures and landscape evolution. Therefore, this study aims at (1) investigating turbulence characteristics of supercritical open-channel flows, (2) conducting hydro-abrasion experiments at the same flow conditions as in (1) to determine the abrasion depths and patterns, and (3) data evaluation and calibration of the abrasion prediction model.

Experimental setup and test program

The experiments were conducted in a $b = 0.2$ m wide, $h = 0.5$ m deep and $l = 13.5$ m long glass and wood-sided laboratory flume with $S_b = 1\%$ bed slope (Fig. 1). The first 5 m of the flume is covered with a non-erodible concrete followed by 6.6 m erodible foam.

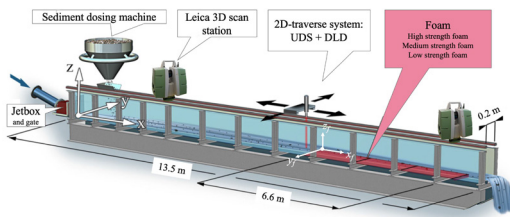


Figure 1. Experimental flume and measuring instruments

Three types of foams with different tensile strengths (f_{st}), compressive strengths (f_c) and Young's modulus (Y_M) were used as bed lining materials (Table 1). The supercritical open channel flow conditions were provided by a gate controlled jetbox system that converts the pressurized conduit flow into the free surface channel flow. The experiments were conducted with flow depths $h_o = 10$ and 20 cm with $F_o = 2, 3$ and 4 at four different sediment supply rates $Q_s = 100, 200, 400$ and 800 g/s (Table 2). Polyurethane foams were placed to the flume bottom with decreasing material strength in the flow direction (Fig. 1). Flow depths were measured using an Ultrasonic Distance Sensor (UDS) and a Distance Laser Device (DLD) mounted on a traverse system consisting. The surfaces of the foams were scanned using a 3D Leica P15 laser scanner after each run with 1 ton of sediment supplied to the flow. The obtained data were used to determine the development of hydro-abrasion pattern and rates.

Table 1. Bed lining material properties

	ρ_s [t/m ³]	f_{st} [MPa]	f_c [MPa]	Y_M [MPa]
Low-strength foam	0.064	0.32	0.36	3.92
Medium-strength foam	0.096	0.50	0.60	5.38
High-strength foam	0.128	0.84	0.92	10.33

Table 2. Experimental matrix

	F_o	b/h_o	S_b	D [mm]	particle	Q_s	material
E1	3	1	1	7.1	sandstone	100, 200, 400, 800	foam 1+2+3
	2	2	1	7.1	sandstone	200	foam 1+2+3
E2	3	2	1	7.1	sandstone	200	foam 1+2+3
	4	2	1	7.1	sandstone	200	foam 1+2+3

Results and discussion

Figure 2 presents the contour maps of final surfaces for the experiments E1 and E2. It shows that hydro-abrasion pattern is dominated by an incision channel along the flume center, growing and enlarging in time. Such pattern is triggered by saltation of bed load particles transported by the flow at the flume center where the bed shear stresses are higher compared to flume side walls. Results also show that for the same amount of sediment transport i.e. 1 ton, the abrasion depths are similar in the two test runs, independent from the sediment supply rate, Froude number, and aspect ratio.

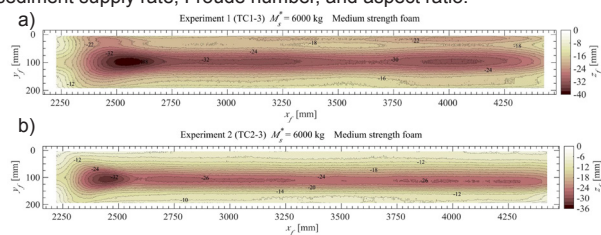


Figure 2. Abrasion pattern on the medium strength foam for a) E1, b) E2

Figure 3a shows the specific gravimetric bedload rate q_s versus the vertical abrasion rate A_v for E1. The abrasion linearly increases with increasing supply rate and it does not reach at a threshold. Fig. 3a also reveals that the abrasion rates decrease with increasing bed lining material strength. The Froude number effect on the abrasion rate A_v is shown in Fig. 3b. A_v increase up to a limit F number and then decreases with increasing F . This behavior is attributed to the reduced energy transfer to the bed per unit meter due to the longer particle hops caused by higher bed shear stresses at high F .

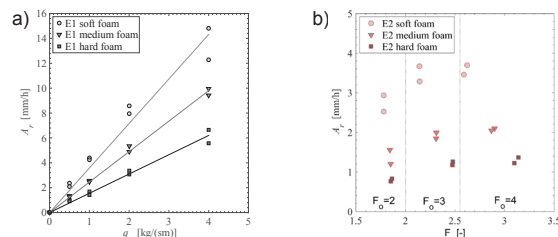


Figure 3. Vertical abrasion rate A_v versus a) bed load mass transport rate per unit width q_s and b) Froude number

Conclusions and outlook

An experimental investigation was conducted to understand the bed abrasion mechanism in supercritical narrow open channel flows existing in hydraulic structures and steep bedrock rivers. Results show that hydro-abrasion develops in the flume center creating a continuous incision channel and such pattern is independent from the Froude number and aspect ratio in the range of $b/h < 2$. Vertical abrasion rate A_v linearly increases with increasing bedload rate, whereas it decreases with increasing bed lining material strength. The Froude number affects the abrasion rate. The findings of this study provide knowledge basis to better understand on hydro-abrasion mechanism and hence lead us to develop a hydro-abrasion prediction model.

References

- Auel, C. (2014). Flow characteristics, particle motion and invert abrasion in sediment bypass tunnels. PhD Thesis, VAW-Mittlung 229 (R. M. Boes, Ed.) Laboratory of Hydraulics, Hydrology and Glaciology, ETH Zurich, Switzerland.
 Auel, C., Albayrak, I., Sumi, T., Boes, R.M. (2017). Sediment transport in high-speed flows over a fixed bed: 2. Particle impacts and abrasion prediction. *Earth Surface Processes and Landforms*, 42(9), 1384-1396.
 Müller-Hagmann, M. (2017). Hydroabrasion by High-Speed Sediment-Laden Flows in Sediment Bypass Tunnels. VAW-Mittlung 239 (R.M. Boes, Ed.), Laboratory of Hydraulics, Hydrology and Glaciology, ETH Zurich, Switzerland.
 Scheingross, J.S., Brun, F., Lo, D.Y., Omerdin, K., Lamb, M.P. (2014). Experimental evidence for fluvial bedrock incision by suspended and bedload sediment. *Geology*, 42(6), 811-815.
 Sklar, L.S., Dietrich, W.E. (2001). Sediment and rock strength controls on river incision into bedrock. *Geology*, 29(12), 1153-1157.

Seismic behavior of Pine Flat concrete gravity dam using microplane damage-plasticity model



Samuel Vorlet, Pedro Manso, Giovanni De Cesare
 Platform of Hydraulic Constructions (PL-LCH), Ecole Polytechnique Fédérale de Lausanne (EPFL)



Introduction

The response of gravity dams under seismic loads is a major concern of dam safety assessment in earthquake-prone areas. The dynamic response of the dam body depends to some extent on the binding foundation conditions as well as on the interaction with the reservoir. During earthquakes, gravity dams are subject to strong horizontal and vertical motions inducing stresses with peaks that may be greater than the maximal strength and consequently lead to damage in the dam body, mainly in tension state. Currently, most dam safety evaluations with finite elements (FE) analysis of reservoir-dam-foundation systems consider a linear elastic model for mass concrete with failure criteria based on maximal tensile strength [1,2], in particular for the non-extreme load combinations. First assessments of extreme load combinations using linear analyses allow preliminary estimates of the location and extent of tensile stress peaks greater than the maximal concrete tensile strength but cannot inform on stress and stiffness redistribution during an earthquake (damage time evolution). This study concerns linear and nonlinear analyses with damage model in order to assess the dam safety under seismic loads resulting with stress peaks leading to damage in the dam body. It presents the seismic analysis of Pine Flat Dam for the 15th International Benchmark Workshop on Numerical Analysis of Dams to be held in Milan in September 2019. It focuses on the tallest non-overflow monolith of Pine Flat concrete gravity dam located on King's River, east of Fresno, California (USA).

Methods

Numerical simulations were performed using the finite element code ANSYS (M-APDL) to discretize the governing equations on the computational domain. A two-dimensional finite elements (FE) model of the reservoir-dam-foundation system is considered. The dam is composed of 37 monoliths and its crest is 561 m long. The tallest non-overflow monolith is 121.91 m high with a 95.8 m base length. The dam body and rock foundation (700 m x 122 m) are modeled with quadrilateral structural plane strain elements. The reservoir is modeled using acoustic elements with inviscid and compressible.

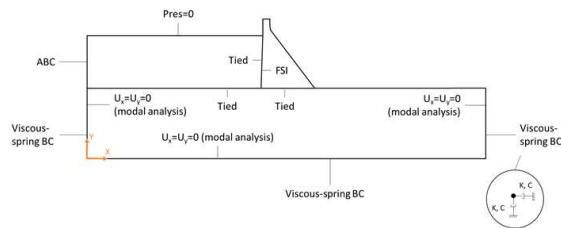


Figure 1: Reservoir-dam-foundation FE model boundary conditions and interfaces

For damage modeling in the dam body, a coupled damage-plasticity model for concrete [3] based on microplane formulation [4, 5] is used. The model has the ability to define different damage initiation criteria and damage evolution laws between tension and compression states. The model can additionally represent cyclic loading conditions, where stiffness lost during cracking is recovered due to crack closure during transition from tension to compression state, while damage sustained under compression remains upon transition to tension state [3].

Dynamic properties

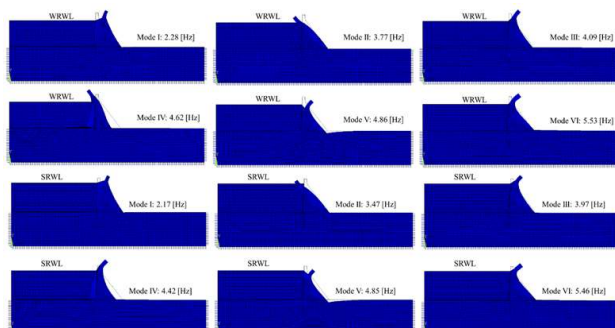


Figure 2: Natural frequencies and mode shapes; Winter Reservoir Water Level (WRWL); Summer Reservoir Water Level (SRWL)

Linear analysis

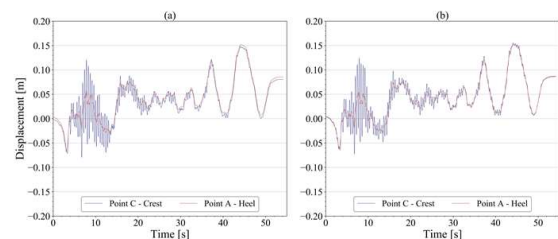


Figure 3: Computed horizontal displacements at crest and heel of the dam; (a) WRWL; (b) SRWL; Taft Record acceleration

Nonlinear analysis

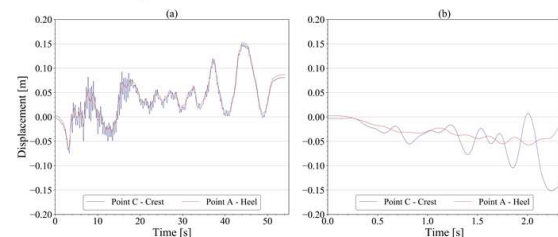


Figure 4: Computed horizontal displacements at crest and heel of the dam; (a) Taft Record acceleration, no failure; (b) artificially designed ETAF acceleration, failure

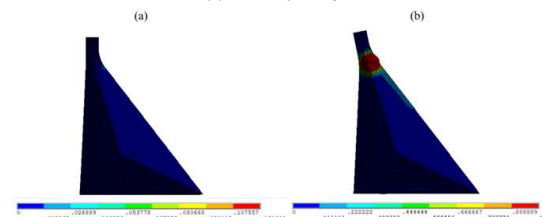


Figure 5: Computed damage parameter DMG; (a) Taft Record acceleration, no local dam failure; (b) artificially designed ETAF acceleration, failure of the dam body

Conclusions

Results show the ability of the numerical models to: (i) reproduce adequately the dynamic properties of the reservoir-dam-foundation system and (ii) conduct dynamic linear and nonlinear analysis. Results of nonlinear analyses show the ability of the model to represent cyclic loading conditions, with recovery of the stiffness lost during cracking in the transition from tension to compression state, and subsequent failure of the dam body near the crest.

References

- [1] Calayir Y., Karaton, M. (2005). A continuum damage concrete model for earthquake analysis of concrete gravity dam-reservoir systems. *Soil Dynamics and Earthquake Engineering*, Vol. 25(11), pp. 857-869.
- [2] Brühwiler E., Wittmann F. (1990). Failure of dam concrete subjected to seismic loading conditions. *Engineering Fracture Mechanics*, Vol. 35(1/2/3), pp. 565-571.
- [3] Zreid I., Kaliske M. (2018). A gradient enhanced plasticity-damage microplane model for concrete. *Computational Mechanics*, Vol. 62(15).
- [4] Bazant Z., Bambarova P. (1984). Crack shear in concrete: crack band microplane model. *Journal of Structural Engineering*, Vol. 10(19), pp.201-2035
- [5] Bazant Z., Oh B. (1985). Microplane model for progressive fracture of concrete and rock. *Journal of Engineering Mechanics*, Vol. 11(115), pp.559-582